Optimization Study of Survey Line Deployment Strategies in Multi-Beam Bathymetric Technology

Houyong Wang, *Member, IAENG,* Qiang Zhang, Jiedong Lan, Zhengxiong Zhu

***Abstract*—Multi-beam bathymetric technology represents an efficient means for measuring underwater terrain, furnishing more detailed depth information compared to single-beam bathymetry. However, optimizing the deployment of survey lines to achieve high efficiency and precision remains a crucial challenge. This paper endeavors to optimize the surveying process by formulating mathematical models and optimization algorithms for the coverage width and overlap rate in multi-beam bathymetry, with the aim of minimizing the length of survey lines. The research is carried out in three consecutive stages. In the initial stage, a mathematical model for the multi-beam coverage width and overlap rate is constructed, leveraging the geometric relationships inherent in an ideal sloping seafloor. Subsequently, the model is enhanced by permitting the horizontal projection angle between the survey line direction and the seabed slope normal to be arbitrary. The coverage width model is further refined through the clarification of geometric relationships. Finally, in the case of complex seafloor terrains, the entire sea area is partitioned into several survey zones, each of which is approximated as a regular sloped plane, to develop a single-objective optimization model for the exploration of survey line deployment. By solving the models with MATLAB, computed results for water depth, coverage width, and overlap rate under diverse conditions are obtained, and the survey line deployment plan is visualized. This study successfully constructs an optimization model for multi-beam bathymetry and validates its effectiveness through examples, providing a theoretical foundation and practical guidance for actual marine surveying, thereby contributing to the improvement of the efficiency and accuracy of marine mapping.**

***Index Terms*—Multi-beam Bathymetry, survey line layout, projection principle, recursive traversal algorithm, single-objective optimization**

I. Introduction

SEABED depth measurement, an essential and significant branch within the realm of oceanographic research, encompasses multiple diverse fields, including marine geology, marine ecology, seabed resource exploration, and marine engineering construction. Serving as a fundamental and crucial task in the domain of ocean science, seabed depth measurement garners high regard and significance on a global scale. The multibeam bathymetric system, which plays a pivotal role in this regard, is illustrated in Fig. 1.

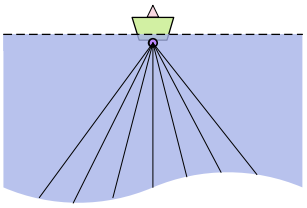

Fig. 1. The Working Principle of the Multi-Beam Bathymetric System

Cheng et al. [1] ensured the attainment of bathymetric data meeting the predefined topographic resolution requirements by gradually optimizing the design while ensuring full-coverage measurements and maintaining high measurement efficiency. He et al. [2] proposed a multi-beam bathymetric system integrating advanced technologies, enhancing the operational efficiency and measurement accuracy of sea-sweeping projects through innovative survey line laying, sensor calibration, and high-precision data processing. Dong et al. [3] introduced a set of methods for analyzing and processing concave and convex deformed terrain in multi-beam systems, including real-time identification and correction of terrain anomalies and transducer deviations, effectively improving the accuracy and reliability of seafloor terrain measurement. Zhang et al. [4] emphasized the importance and urgency of enhancing the accuracy, coverage, water body detection ability, and simplifying the data processing in seafloor bathymetry. Mi [7] proposed a method to efficiently acquire underwater topographic information using a multi-beam system and GNSS-RTK on an unmanned vessel. Yang et al. [8] verified the high efficiency and accuracy of a combined system in underwater structure detection, demonstrating its advantages through actual cases and providing new technical means for related engineering. Han [9] combined various data to formulate detailed principles and preplans for survey line deployment to ensure data quality and survey efficiency. Zhu [10] suggested the use of discrete point cloud data interpolation and fitting in multi-beam ocean mapping and considering relevant factors in algorithm selection. Liu [11] analyzed key factors affecting multi-beam measurement accuracy and proposed comprehensive quality assurance

Manuscript received May 3, 2024; revised November 21, 2024.

Houyong Wang is an undergraduate student at School of Automobile and Traffic Engineering, Wuhan University of Science and Technology, Wuhan 430065, China (e-mail:18635851547@163.com).

Qiang Zhang is a lecturer at College of Science, Wuhan University of Science and Technology, Wuhan 430065, China (corresponding author to provide phone: +86-15271930390; e-mail: zhangqiang@wust.edu.cn).

Jiedong Lan is an undergraduate student at School of Automobile and Traffic Engineering, Wuhan University of Science and Technology, Wuhan 430065, China (e-mail: jiedong_l@163.com).

Zhengxiong Zhu is an undergraduate student at School of Automobile and Traffic Engineering, Wuhan University of Science and Technology, Wuhan 430065, China (e-mail: 17740589915@163.com).

measures, such as using the RTK-DGPS system. Wang [12] proposed a multi-beam survey method based on AUVs' constant depth mode, achieving successful surveys in unfamiliar waters with significantly improved operational efficiency. Wang et al. [13] designed a line-laying system for polar ocean surveys, improving the efficiency of multi-beam survey program design. Shan et al. [14] found a strong correlation between gravity data complexity and survey line density, guiding ship survey route design. Xu [15] applied a multi-beam system to measure sediment in a harbor channel, providing support for navigation safety and disaster response. Zhang et al. [16] proposed a new algorithm for survey line laying and trajectory control to ensure efficient data collection. Chai [17] proposed strategies for survey line laying, including controlling the intersection angle and mileage of check lines. Shi et al. [18] combined prior knowledge to optimize the denoising process and improve data processing speed and accuracy. Xia et al. [19] pointed out the effects of survey line laying direction on seabed topography display and proposed suitable laying methods for different terrains. Xiao [20] proposed a high-precision positioning method for seafloor datums, compensating for sound velocity errors and improving underwater positioning. Cheng et al. [21] proposed an optimization method for survey line placement based on side-scan sonar resolution, improving seafloor target detection. Bai et al. [22] used a segmented scanning method to avoid steep sections in survey line planning, benefiting seismic exploration. Jin et al. [23] proposed a method to estimate marine gravity survey line spacing using a global gravity field model, reducing workload and improving efficiency. Qi et al. [24] proposed a data thinning algorithm considering slope and elevation, improving the accuracy and feature retention of thinned data. Yu [25] obtained a high-precision underwater 3D model using a combined system. Zhou et al. [26] achieved high-precision correction of ALB bathymetry data with a neural network model. Xue [27] proposed an improved algorithm for constructing seafloor terrain models, enhancing efficiency and quality. Li's research [28] emphasized the combination of appropriate bathymetric technologies to optimize marine surveying and mapping.

The research efforts of the aforementioned authors predominantly focus on enhancing the accuracy and efficiency of marine surveying and mapping, with particular emphasis on seabed topographic surveying. Their specific approaches encompass optimizing survey line laying principles, enhancing multi-beam bathymetric systems, devising new data processing techniques and algorithms, and leveraging advanced electronic, computer, and satellite positioning technologies.

Nevertheless, as a crucial element in the technical design of maritime zones, the design methodology of survey line laying remains relatively antiquated, and its implementation process is convoluted. In practical applications, it encounters issues such as high costs, complex operations, or a high technical threshold. Additionally, there is a paucity of studies on the long-term stability and reliability of new technologies and methods, necessitating continuous observation and evaluation in practical scenarios.

In light of this situation, this paper proposes a multi-beam survey line deployment method based on "prior bathymetric" measurement. Through in-depth analysis of how survey line deployment impacts measurement results, this method capitalizes on historical measurement data to optimize the survey line layout during the measurement process. It effectively augments measurement efficiency and accuracy while reducing the number of survey lines and measurement time, presenting significant advantages over the traditional "equal distance deployment method."

Specifically, this paper tackles the aforementioned problem via the following aspects:

1) Minimizing the total length of survey lines via mathematical modeling and optimization algorithms, thereby cutting costs.

2) Enhancing measurement efficiency by optimizing the survey line layout and segmenting the measurement of complex sea areas, thus streamlining the implementation process and reducing the technical threshold.

3) MATLAB programming for model solving and result visualization, which can boost the technology's operability.

4) Verifying the model's validity through practical cases to evaluate the new technology's stability and reliability.

Section 2 presents the research idea and hypothesis. Section 3 details the research process, results, and discussion. Section 4 concludes the study.

II. Research Methods

This paper will present the entire process of measuring the depth of seawater using multi-beam lines, from simple to complex:

In Phase 1, when the seafloor is a sloped plane with a slope of α and the projection angle between the survey line direction and the normal direction of the seafloor slope on the horizontal plane is $\beta = 90°$, a mathematical model for the coverage width and overlap rate in multi-beam bathymetry is to be established.

In Phase 2, given a sloped seabed with slope α and an arbitrary angle β between the survey line direction and the horizontal projection of the seabed slope normal, a mathematical model for the coverage width of multi-beam bathymetry is to be formulated.

In Phase 3, for seabeds with irregular shapes, a survey line layout is to be designed to fulfill the following requirements:

1) The strip formed by scanning along the survey line should cover the entire area to be measured as comprehensively as possible;

2) The overlap rate between adjacent strips should be maintained below 15% whenever feasible;

3) The total length of the survey lines should be minimized.

III. Results and Discussion

In this section, our objective is to develop a mathematical model concerning the coverage width and overlap rate within the context of multi-beam bathymetry, following a three-stage approach.

A. Phase 1: Parallel Survey Lines and Flat Seabed Terrain

The schematic diagram of the measuring line strip of the multi-beam sounding system is shown in Fig. 2:

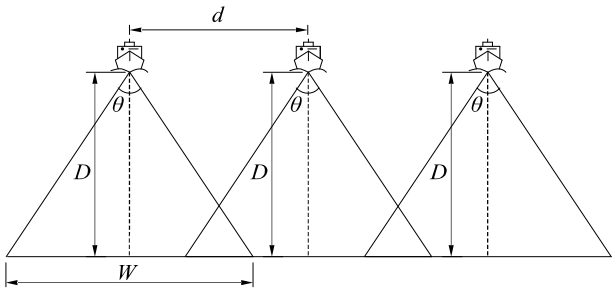

Fig. 2. Schematic Representation of the Measuring Line Strip

In accordance with the geometric principle, the relationship between the coverage width and the seawater depth, as well as the opening angle of the transducer, is presented as follows:

$$W = 2D\tan\frac{\theta}{2} \tag{1}$$

Where, W—— Coverage width of survey lines.
D —— Depth of the sea.
θ —— Opening angle of the multibeam transducer.

The general definition of the overlap rate for adjacent bands is given by the following formula:

$$\eta = \frac{The\ length\ of\ the\ overlapping\ area\ between\ adjacent\ bands}{The\ coverage\ width\ of\ this\ strip} \tag{2}$$

According to the definition of overlap rate between adjacent bands, the relationship between overlap rate and line spacing and coverage width is:

$$\eta = \frac{W-d}{W} = 1-\frac{d}{W} \tag{3}$$

Where, η—— Overlap rate of line coverage width.
d—— The distance between two adjacent survey lines.

The relationship between the overlap rate and the distance between the measuring lines, the depth of seawater, and the opening angle of the transducer is further obtained as follows:

$$\eta = 1-\frac{d}{2D\tan\frac{\theta}{2}} \tag{4}$$

Next, we will further investigate the coverage width of multi-beam bathymetry and the overlap rate between adjacent bands when the seabed slope is not 0.

B. Phase 1: Parallel Survey Lines and Uneven Seabed Terrain

1) Establishment of model

The schematic diagram of two adjacent survey lines in the multi-beam sounding system is depicted in Fig. 3:

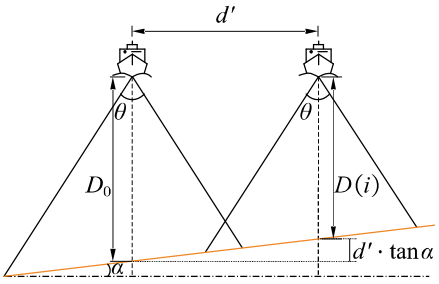

Fig. 3. Schematic Diagram of Two Parallel Measuring Line Strips

According to the theory of right angled triangles and trigonometric functions, the relationship between the depth of seawater D_i corresponding to measuring lines at different distances from the center of the sea area and the depth of seawater D_0 corresponding to measuring lines passing through the center of the sea area is:

$$D(i) = D_0 + d'\tan\alpha \tag{5}$$

Among them, i is a positive integer, and d' represents the distance of the measuring lines from the center point of the sea area, with negative values indicating the west side and positive values the east side. α represents the slope.

The schematic diagram of the i-th measuring line strip of the multi-beam sounding system is shown in Fig. 4:

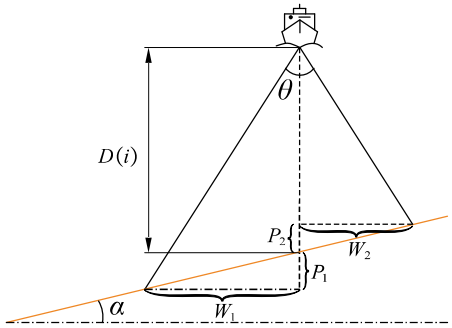

Fig. 4. Cross-Sectional Schematic of the i-Th Measuring Line Strip

According to geometric principles, the relationship between slope, transducer opening angle, seawater depth, and coverage width is:

$$\begin{cases} \tan\alpha = \dfrac{p_1}{W_1} \\ \tan\alpha = \dfrac{p_2}{W_2} \\ \tan\dfrac{\theta}{2} = \dfrac{W_1}{D(i)+p_1} \\ \tan\dfrac{\theta}{2} = \dfrac{W_2}{D(i)-p_2} \end{cases} \tag{6}$$

After simplification and organization, the relationship equations for W_1 and W_2 are obtained as follows:

$$W_1 = \frac{D(i)\tan\frac{\theta}{2}}{1-\tan\alpha\tan\frac{\theta}{2}} \tag{7}$$

$$W_2 = \frac{D(i)\tan\frac{\theta}{2}}{1+\tan\alpha\tan\frac{\theta}{2}} \tag{8}$$

Because $W=W_1+W_2$, the coverage width model for multi-beam bathymetry is obtained:

$$W(i) = \frac{2D(i)\tan\frac{\theta}{2}}{1-\tan^2\alpha\tan^2\frac{\theta}{2}} \tag{9}$$

Among them, i is a positive integer.

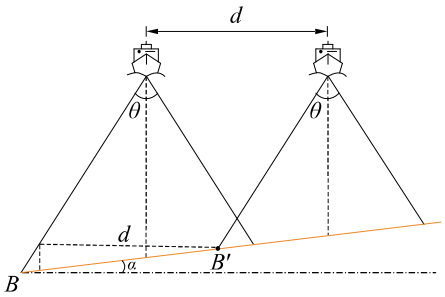

Fig. 5. Profile Schematic of Two Adjacent Measuring Line Strips

According to Fig. 5 and the sine theorem, it can be obtained that the length of the line segment on the slope corresponding to the coverage width of the previous measuring line is:

$$BB' = d \cdot \frac{\sin(90° + \frac{1}{2}\theta)}{\sin(90° - \alpha - \frac{1}{2}\theta)} = \frac{d\cos\frac{1}{2}\theta}{\cos(\alpha + \frac{1}{2}\theta)} \tag{10}$$

Among them, d is the distance between this measuring line and the previous measuring line, θ is the opening angle of the transducer, and α is the slope.

$$\eta = \frac{W - d}{W} \tag{11}$$

According to the general definition Eq.(11) for the overlap rate of adjacent strips, the overlap rate between the coverage width of this measuring line and the coverage width of the previous measuring line when the terrain changes is:

$$\eta = \frac{W(i-1) - BB'\cos\alpha}{W(i)} \tag{12}$$

Substituting Eq.(10) into Eq.(12) , the mathematical model for the overlap rate between the i-th and i-1-th survey lines during terrain undulation changes is:

$$\eta = \frac{W(i-1)}{W(i)} - \frac{d\cos\alpha\cos\frac{1}{2}\theta}{W(i)\cos(\alpha + \frac{1}{2}\theta)} \tag{13}$$

2) Solving the model

Assuming the opening angle of the multi-beam transducer is 120°, the seabed slope is 1.5°, and the depth of seawater at the center point of the sea area is 70 m. The depth calculation model for seawater is Eq.(5), the coverage width calculation model is Eq.(9), and the overlap rate calculation model with the previous measurement line is Eq.(13), the initial conditions are:

$$\begin{cases} \theta = 120° \\ \alpha = 1.5° \\ D_0 = 70 \end{cases} \tag{14}$$

The objective function is:

$$\begin{cases} D(i) = D_0 + d'\tan\alpha \\ W(i) = \dfrac{2D(i)\tan\frac{\theta}{2}}{1 - \tan^2\alpha\tan^2\frac{\theta}{2}} \\ \eta = \dfrac{W(i-1)}{W(i)} - \dfrac{d\cos\alpha\cos\frac{1}{2}\theta}{W(i)\cos(\alpha + \frac{1}{2}\theta)} \end{cases} \tag{15}$$

This paper employs MATLAB to solve the proposed model. The corresponding algorithm flowchart is illustrated in Fig. 6, and examples of the solution results are presented in TABLE I.

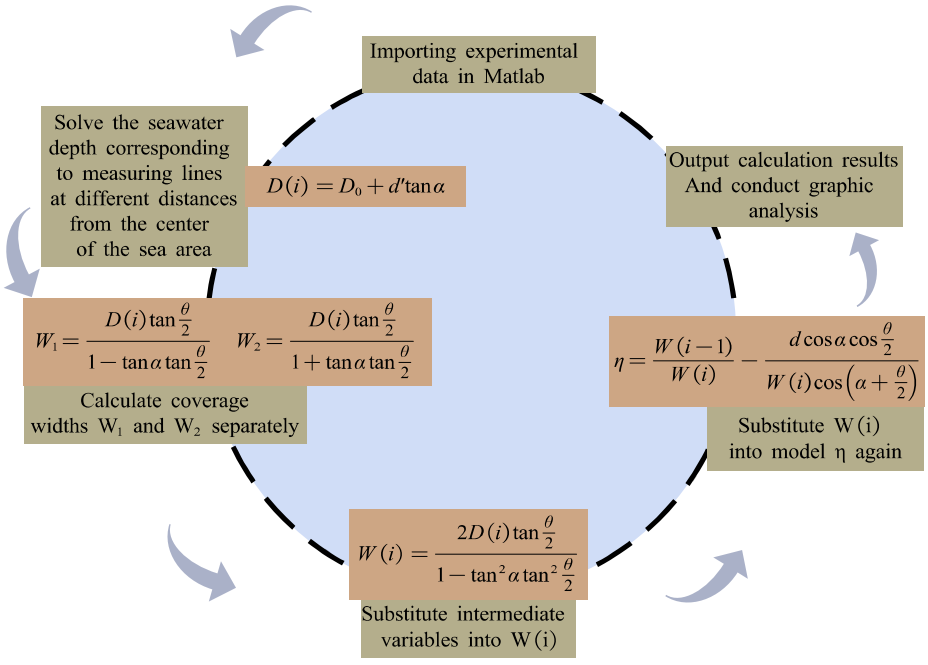

Fig. 6. Flowchart of the Solution in Phase 1

3) Result analysis

1) **Seawater depth:** The seawater depth at diverse locations diminishes as the distance between the survey line and the center point increases, and the rate of decrease is proportional to tanα. It is evident that the depth of the sea is solely related to the depth at the center of the sea, denoted as D_0, and the slope α of the seabed. This relationship can be observed in Fig. 7.

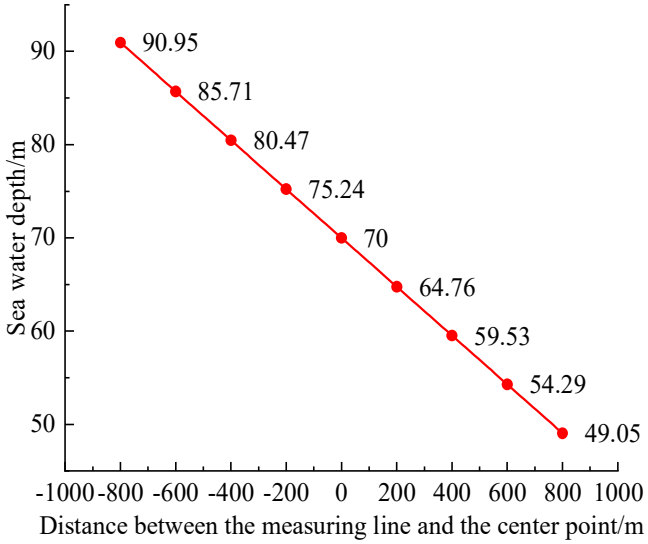

Fig. 7. Relationship between Sea Depth and the Distance of the Survey Line from the Center Point

2) **Coverage width:** The coverage width in multi-beam measurement shows a concordant changing trend with that of the seawater depth, decreasing as the latter decreases. This implies that, with constant measurement line spacing and transducer opening angle, the coverage width of the multi-beam instrument is narrower in shallow water areas, as observable in Fig. 8.

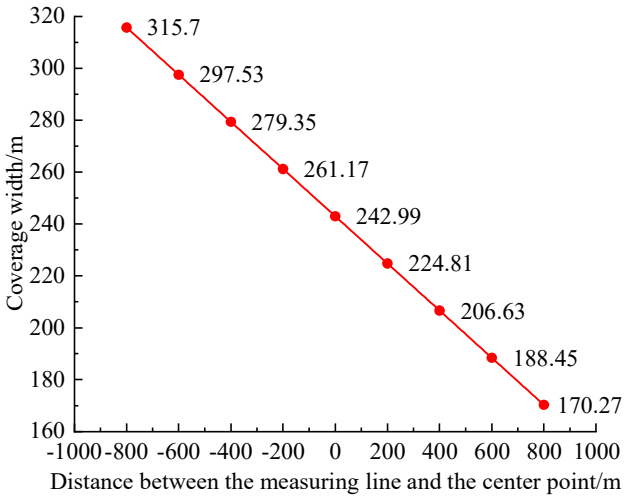

Fig. 8. Relationship between Coverage Width and the Distance from the Center Point of the Measuring Line

3) **Overlap rate:** As shown in TABLE I, in deeper seawater, the overlap rate between adjacent bands is relatively high, ensuring full coverage but at the cost of lower efficiency. Conversely, in shallower water, the overlap rate is small or even negative, causing measurement gaps. Thus, in deep water areas, increasing the survey line spacing can enhance measurement efficiency, while in shallow water areas, more survey lines should be employed to achieve full coverage. This is illustrated in Fig. 9.

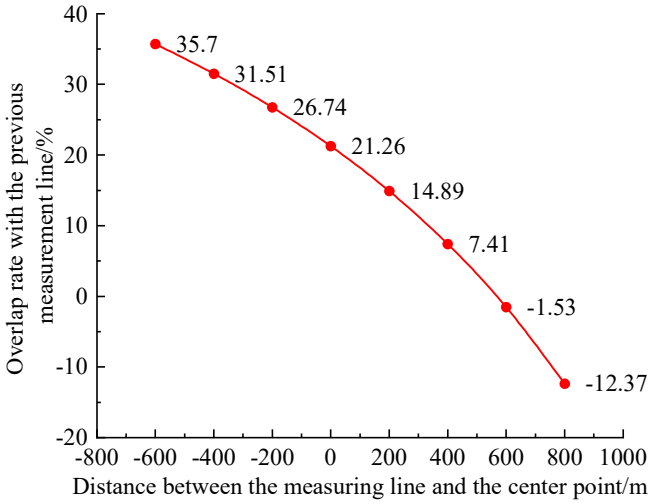

Fig. 9. Relationship between Overlap Rate and the Distance between the Measuring Line and the Center Point

4) Analysis of influencing factors

Using the control variable method to study coverage width w and overlap rate η relationship with various parameters.

1) The impact of opening angle of multi-beam transducer θ on coverage width (Fig. 11 (a)): Controlling seabed slope α、the distance between measuring lines and other factors remain unchanged, and only the opening angle of the transducer is adjusted θ。

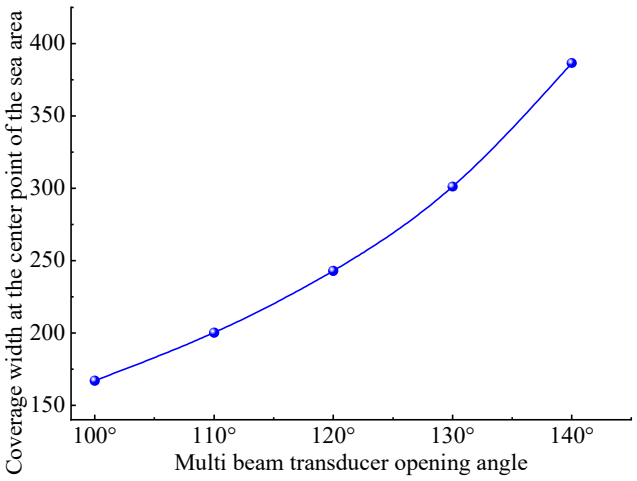

Fig. 10. Relationship between the Opening Angle of the Transducer and the Coverage Width at the Center of the Sea Area

Fig. 10 depicts the variation curve of the coverage width at the center of the sea area under different transducer opening angles θ. It is evident that as the opening angle increases, the coverage width also increases, with an increasing growth rate. Moreover, for a specific θ, the coverage width decreases as the distance between the survey line and the center point increases, meaning that in shallower seawater, the coverage width is smaller, exhibiting a linear relationship.

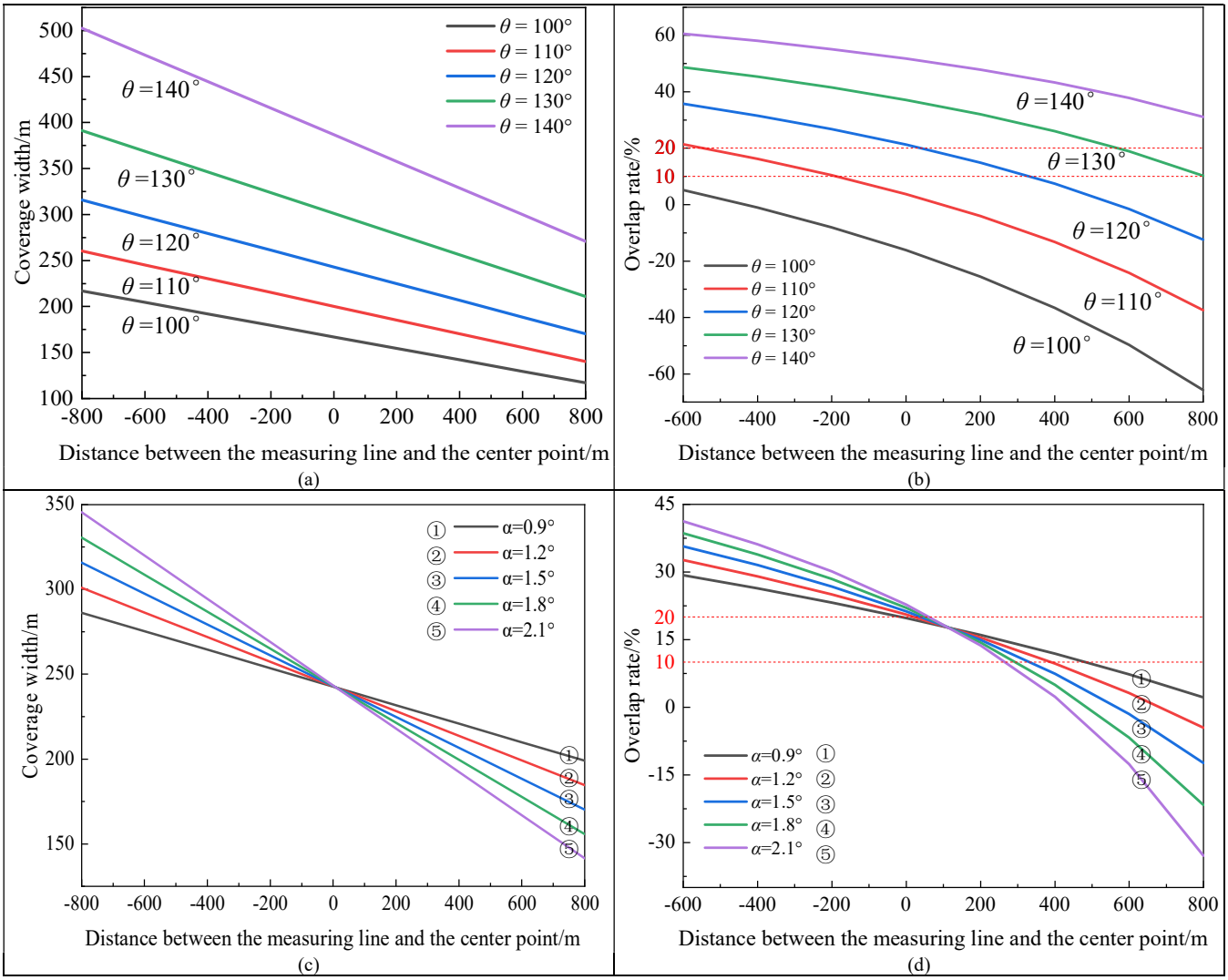

Fig. 11. Influence Curves of the Opening Angle and Seabed Slope of the Multi-Beam Transducer on the Beam Coverage Width and Overlap Rate, Respectively

2) The influence of the multi-beam transducer's opening angle θ on the overlap ratio (Fig. 11(b)): By keeping factors like the seafloor slope α and survey line spacing d constant and only adjusting the transducer's opening angle θ, it is observable from the figure that as the opening angle increases, the overlap ratio continuously rises. Moreover, a larger opening angle leads to a greater distance from the center point to the survey line that meets the overlap ratio range condition (10% - 20%). Additionally, for a specific θ, as the distance from the center point along the survey line increases, the overlap ratio decreases, i.e., the shallower the seawater, the smaller the overlap ratio, suggesting that under-measurement may occur in shallow water areas.

3) The impact of seafloor slope α on the coverage width (Fig. 11(c)): While keeping the transducer opening angle θ and survey line spacing d constant, only the seafloor slope α is adjusted.

Fig. 12 shows the change curve of the coverage width at the center of the sea area for different seafloor slopes α. It is evident from the figure that as the seafloor slope α rises, the coverage width continuously increases with an accelerating growth rate, though the overall increase is not significant.

4) The impact of seafloor slope α on the overlap ratio (Fig. 11(d)): Keeping the transducer opening angle θ and survey line spacing d constant and only adjusting the seafloor slope α, it can be seen from the figure that to the left of the centerline, the seafloor slope is positively correlated with the overlap rate, while to the right of the centerline, it is negatively correlated. Moreover, the larger the slope α, the smaller the distance from the line to the center of the centroid that meets the overlap rate conditions.

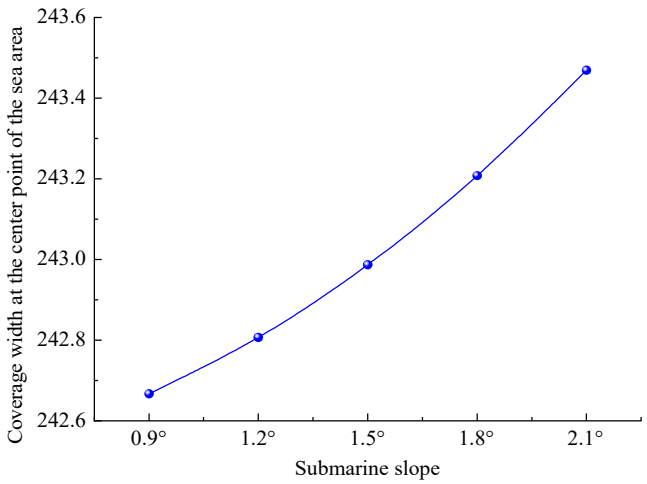

Fig. 12. Relationship between Seafloor Slope and the Coverage Width at the Center of the Sea Area

5) The influence of survey line spacing d on the overlap ratio (Fig. 13): With the transducer opening angle θ, seafloor slope α, and other factors held constant, only adjust the survey line spacing d.

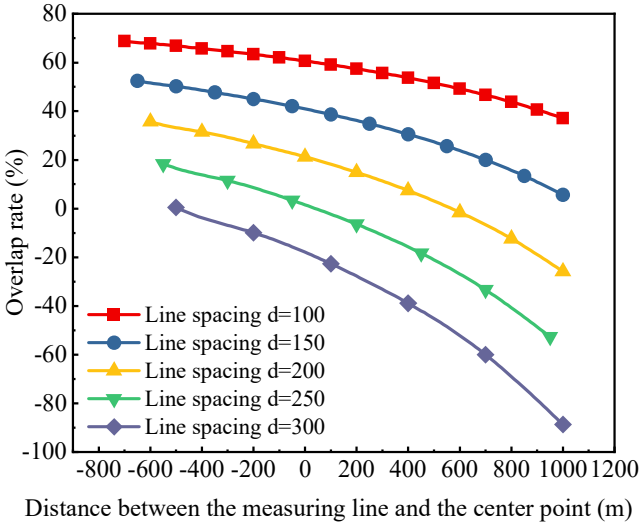

Fig. 13. Overlap Ratio at Different Survey Line Spacings

As can be seen from the figure, as the survey line spacing d increases, the overlap ratio decreases; As shown in Fig. 14, the smaller the overlap ratio, it indicates that the under-measurement range compared to the previous survey line is gradually increasing. (The simulation schematic is shown in Fig. 14).

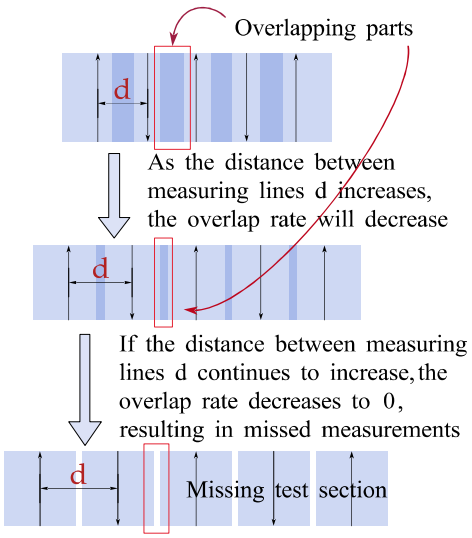

Fig. 14. Schematic Diagram of Overlap Ratio Variation

C. Phase 2

1) Establishment of model

In the rectangular sea area designated for surveying, β denotes the angle between the survey line direction and the horizontal projection of the slope's normal. Firstly, given the slope of the seawater is α and the distance between the measuring ship and the center point of the sea area is e, the seawater depth remains invariant with respect to β. The angle between the horizontal plane and the line segment formed by the intersection of the multibeam plane and the seabed slope is no longer α and requires adjustment, as presented in the following equation:

$$D' = D_0 + e\cos\beta\tan\alpha \tag{16}$$

The following is the derivation process of the D→D' adjustment (This can be seen in Fig. 15):

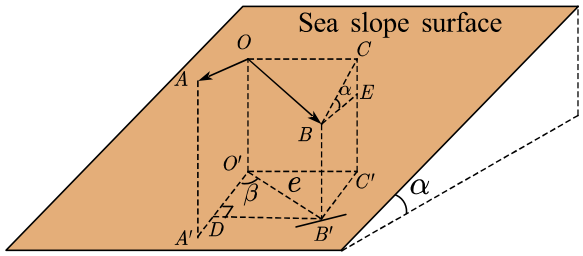

Fig. 15. Geometric Relationship Diagram of Sea Water Depth

O'A' is the projection of the normal direction of the slope in the horizontal plane, O'B' is the projection of the ship survey line in the horizontal plane, OA and OB is O'A′, O'B′ are projections falling on the slope surface, where ∠A′O′B′ =β, the perpendicular line of O′A′ is crossed by B′, the perpendicular foot is D, and the quadrilateral O′A′B′C′ is rectangular, so B′C′ = A′O′ = e·cosβ, because B′C′ parallel to BE, so BE=B′C′=e · cos β , in ΔBCE, ∠CBE=α, so CE=e·cosβtanα, CE is the depth of increase or decrease, plus the depth of the sea water in the center of the sea D_0, then the final adjusted sea depth is the Eq.(16).

The slope correction after incorporating the angle β is:

$$\alpha' = \arctan(\tan\alpha \cdot \sin\beta) \tag{17}$$

Here's how α' is derived:

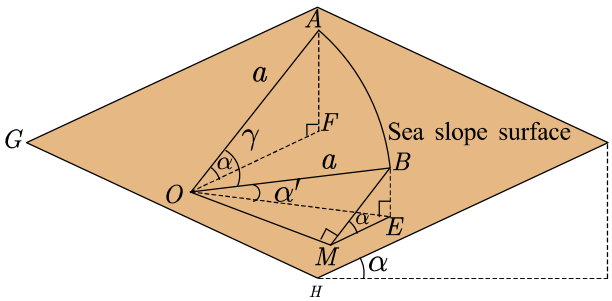

Fig. 16. Schematic Diagram for Derivation

As shown in Fig. 16, OA is the straight line of the normal projection of the slope surface falling on the slope surface, OA obtains OB by rotating the angle γ the slope surface, OB is the intersection line between the beam plane and the sea slope surface, OA and OB are both on the sea slope, and then it is projected to the horizontal plane to obtain OF and OE, the slope is α, then ∠AOF = α, rotation angle ∠AOB = γ, assuming OA=OB=a, the slope is required to be adjusted ∠BOE = α', make BM perpendicular to OM at point B, the vertical foot is the point M, and the EM is connected, then

The relationship between the angles of two intersecting lines in space and the horizontal angles of their projections is obtained:

$$\cos\gamma = \sin\alpha'\sin\alpha + \cos\alpha'\cos\alpha\cos\angle FOE \tag{18}$$

Derived from geometric principles:

$$\angle FOE = \frac{\pi}{2} - \beta \tag{19}$$

Arranged to obtain:

$$\cos\gamma = \sin\alpha'\sin\alpha + \cos\alpha'\cos\alpha\sin\beta \tag{20}$$

In the right triangle OMB,

$$MB = a\sin\angle MOB = a\sin(\frac{\pi}{2} - \gamma) = a\cos\gamma \tag{21}$$

In the right triangle MEB,

$$BE = MB\sin\alpha \tag{22}$$

Also in the right triangle OEB,

$$\sin\alpha' = \frac{BE}{a} = \sin\alpha'\sin^2\alpha + \cos\alpha'\cos\alpha\sin\beta\sin\alpha \tag{23}$$

To put it simply:

$$\tan\alpha' = \tan\alpha\sin\beta \tag{24}$$

Namely:

$$\alpha' = \arctan(\tan\alpha \cdot \sin\beta) \tag{25}$$

Then, Eq.(16) and Eq.(25) are substituted into the refined expression for coverage width:

$$W = \frac{2D'\tan\frac{\theta}{2}}{1 - \tan^2\alpha'\tan^2\frac{\theta}{2}} \tag{26}$$

Obtaining the multi-beam bathymetric coverage width model when the angle between the survey line direction and the normal to the seafloor slope, projected on the horizontal plane, is an arbitrary angle:

$$W = \frac{2\tan\frac{\theta}{2}(D_0 + e\cos\beta\tan\alpha)}{1 - \tan^2\alpha\sin^2\beta\tan^2\frac{\theta}{2}} \tag{27}$$

2) Solving the model

It is known that the opening angle of the multi-beam transducer is θ =120°, the slope is α =1.5°, and the sea depth at the center point of the sea area is 120m.

The objective function is:

$$W = \frac{2\tan\frac{\theta}{2}(D_0 + e\cos\beta\tan\alpha)}{1 - \tan^2\alpha\sin^2\beta\tan^2\frac{\theta}{2}} \tag{28}$$

The initial conditions are:

$$\begin{cases} \theta = 120° \\ \alpha = 1.5° \\ D_0 = 120m \\ e = 0, 0.3, 0.6, 0.9, 1.2, 1.5, 1.8, 2.1 \\ \beta = 0°, 45°, 90°, 135°, 180°, 225°, 270°, 315° \end{cases} \tag{29}$$

In this paper, Matlab is used to solve the model. The results are shown in TABLE II and visualized in Fig. 17.

3) Result analysis

When the angle between the survey direction is within 0° - 90° (excluding 90°), the coverage width increases as the distance between the survey ship and the center point of the sea area increases. When the angle of the survey line direction is 90°, regardless of the distance of the measurement ship from the center point of the sea area, the coverage width remains equal. For the angle between the survey direction within 90° - 270° (excluding 90° and 270°), the coverage width decreases with the increase in the distance between the survey ship and the center point. When the survey direction angle is 270°, the coverage width of the measurement ship at any distance from the center point is equal and consistent with that when the survey line direction angle is 90°. When the angle between the survey direction is within 270° - 360° (excluding 270°), the coverage width increases as the distance between the survey ship and the center point of the sea area increases.

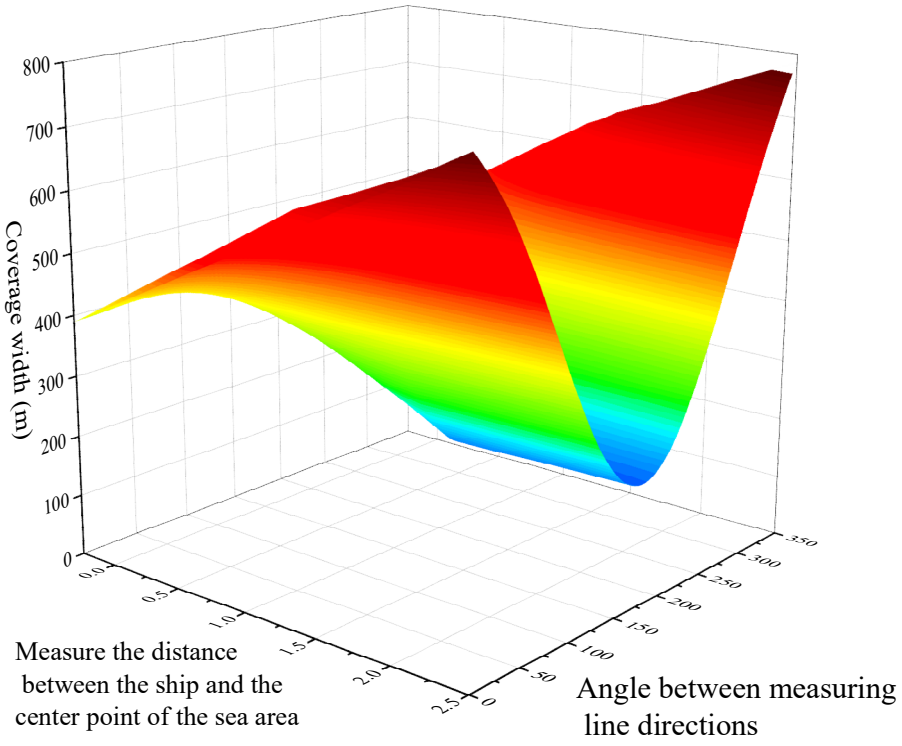

Fig. 17. Schematic Diagram of the Coverage Width of Multi-Beam Bathymetry at Various Locations

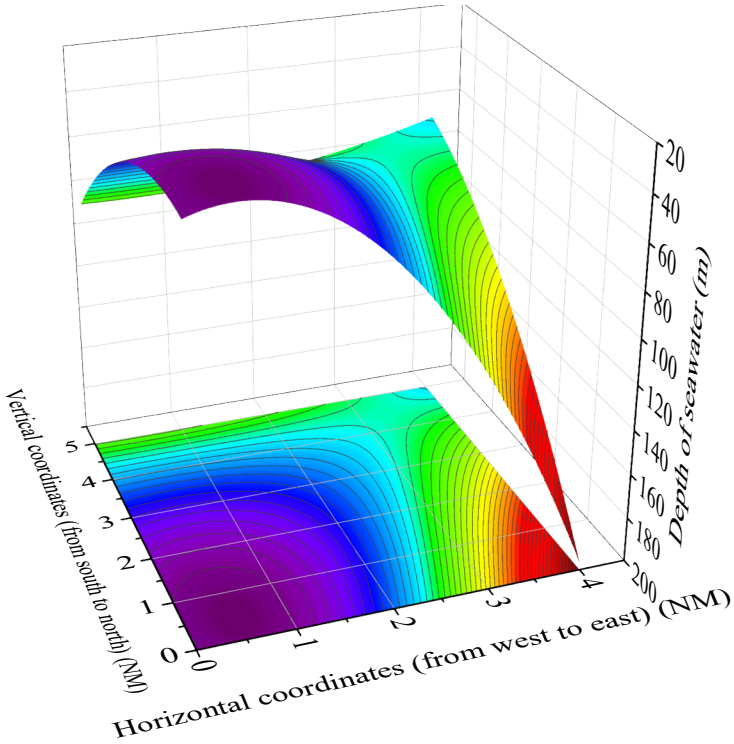

Fig. 18. Three-Dimensional Simulation of the Sea Area Terrain

D. Phase 3: Brief Description of Seafloor Topography

Generally, seafloor topography can change over several years, potentially introducing errors in scientific research relying on seafloor terrain. Thus, we plan survey lines using historical seawater depth data to measure the latest seafloor depth data. The single-beam bathymetric data for a specific sea area (5 nautical miles long and 4 nautical miles wide) measured years ago is shown in TABLE III. Now, we will use this data set as an example to plan survey lines for multi-beam bathymetric survey vessels.

The requirements that need to be met in the design of the survey line layout are as follows:

1) The strip formed by scanning along the survey line should cover the entire area to be measured as comprehensively as possible;

2) The overlap rate between adjacent strips should be maintained below 15% whenever feasible;

3) The total length of the survey lines should be minimized.

E. Phase 3: Design of Survey Line Layout Method

1) Establishment of model

Visualize the seawater depth data as shown in Fig. 18. Due to the significant topographical variations in this sea area, we plan to design the survey lines in a zoned manner.

As illustrated in Fig. 19, in the southwest of the sea area, the contour lines are nearly closed, signifying the highest point of the seafloor terrain, i.e., a protrusion. In the southeast, the contour lines are extremely dense with significant slope changes, indicating a steep slope. In the northeast, the contour lines are sparse and the terrain is relatively flat, which can be regarded as a plane. In the northwest, the contour lines are nearly parallel, which can be considered an ideal slope. Based on this analysis, the survey area can be divided.

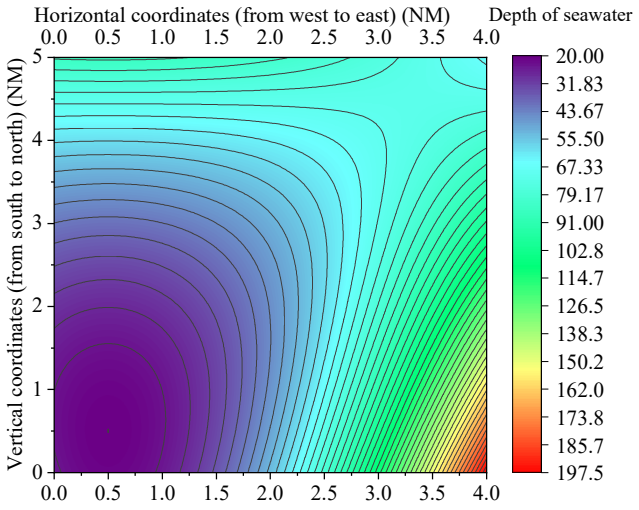

Fig. 19. Contour Map of the Seafloor Topography

The layout of survey lines in the survey area must adhere to certain principles: each survey line should be parallel to each other, [29] and, as much as possible, parallel to the contour lines. [30] Based on these principles, we can divide the area into zones and lay out the survey lines separately in each zone. The division of the survey area is shown in Fig. 20.

Based on the descriptions of the four cardinal directions, the sea area is divided into four survey areas. Then, the seafloor topography of each of the four survey areas is fitted to an ideal inclined plane for processing. This allows the use of the formulas from Phase II to calculate the coverage width and overlap ratio.

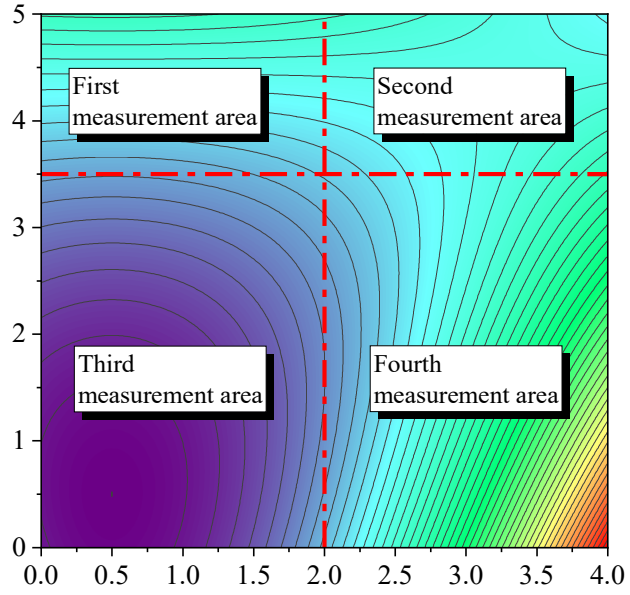

Fig. 20. Division of the Survey Area

We can use a multivariate linear regression model to fit the inclined plane equation. In the spatial coordinate system, assuming the inclined plane equation is $z = A\,x + B\,y + C$, we fit it based on the known seawater depth data. The fitting correlation coefficient $R^2 = 0.9873$, which is very close to an inclined plane, with A = 0.00043194, B = 0.01193957, and C = -28.69.

Then, by geometric relationships, the slope α values of this inclined plane along the x-axis and the y-axis can be obtained:

$$\begin{aligned} \alpha_x &= \arctan A = 0.025° \\ \alpha_y &= \arctan B = 0.68° \end{aligned} \tag{30}$$

For the sake of calculation, and $\alpha_x \ll \alpha_y$, the slope of the slope can be taken as 0.68°

The same method can be used to obtain the inclined plane equations and slope values for the other three survey areas.

Note: Taking the first survey area as an example, the method is the same for the other survey areas.

As shown in Fig. 23, the first survey area has a riverbed that is deep in the north and shallow in the south, therefore, adopting an east-west oriented survey line layout can achieve comprehensive coverage and the shortest total length of survey lines.

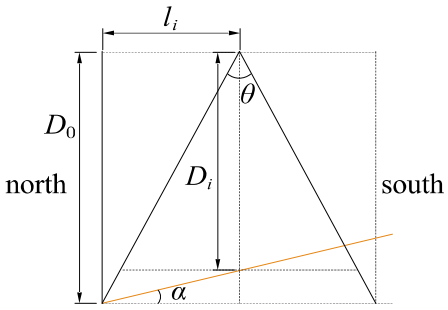

Fig. 21. Geometric Relationship Diagram

When arranging survey lines in an east-west direction, it is necessary to start at the deepest part of the seawater, which is at the northernmost edge. At this time, the distance l_1 from the first survey line on the north side to the north coast needs to be calculated. This can be seen in Fig. 21.

Taking the line where the deepest part of the sea area is located as the initial side, with l_i as the distance from the survey line position to the initial side, d_i as the distance between adjacent survey lines, D_i as the seawater depth at the survey line position, and the known seawater depth D_0 at the initial side, with L_{SN} as the north-south length and L_{EW} as the east-west length of the survey area, the relationship between l_i and the seawater depth D_i can be represented as follows:

$$D_i = D_0 - l_i \tan\alpha \tag{31}$$

The relationship between l_1 and D_0 can be expressed as:

$$l_1 = D_0 \tan\frac{\theta}{2} \tag{32}$$

From Phase 1, it is known that the coverage width of the multi-beam survey line is:

$$W_i = \frac{2D_i \tan\frac{\theta}{2}}{1-\tan^2\alpha\tan^2\frac{\theta}{2}} \tag{33}$$

We take the total length of the survey lines as the minimum optimization target and establish a single-objective optimization model with two constraints: to cover the entire area to be surveyed and the adjacent swaths as much as possible, and to control the overlap ratio between 15% and below.

$$\min nL_{EW} \tag{34}$$

$$s.t.\begin{cases} \sum_{i=1}^{n} W_i - \sum_{i=1}^{n-1} W_i\eta_i \geq L_{SN} \\ \eta_i \leq 20\% \end{cases} \tag{35}$$

Thereinto:

$$\begin{cases} W_i = \dfrac{2D_i \tan\frac{\theta}{2}}{1-\tan^2\alpha\tan^2\frac{\theta}{2}} \\ \eta_i = 1 - \dfrac{d_i\cos\alpha\cos\frac{1}{2}\theta}{W_i\cos(\alpha+\frac{1}{2}\theta)} \\ D_i = D_0 - l_i\tan\alpha \\ l_{i+1} = l_i + d_i \\ l_1 = D_0\tan\dfrac{\theta}{2} \end{cases} \tag{36}$$

2) Solving the model

In the first survey area, the following conditions are known:

$$\begin{aligned} L_{EW} &= (4-2)\times 1852 \\ L_{SN} &= (5-3.5)\times 1852 \\ \alpha &= 0.68° \\ \theta &= 120° \\ D_0 &= 83.86 \end{aligned} \tag{37}$$

Simultaneously, to ensure the convenience of measurement and the completeness of data, there should be an overlap ratio of 10% to 15% between adjacent swaths. To minimize the total length, a lower overlap ratio is preferred, which can be set at 10%, that is:

$$\eta_i = 10\% \tag{38}$$

The calculated distance l_1 from the first survey line on the north side to the north coast is 145.2498 meters, and a total of 14 survey lines are planned in the first survey area. The

parameters of the line layout are shown in TABLE IV. The layout of the survey line is shown schematically in Fig. 22.

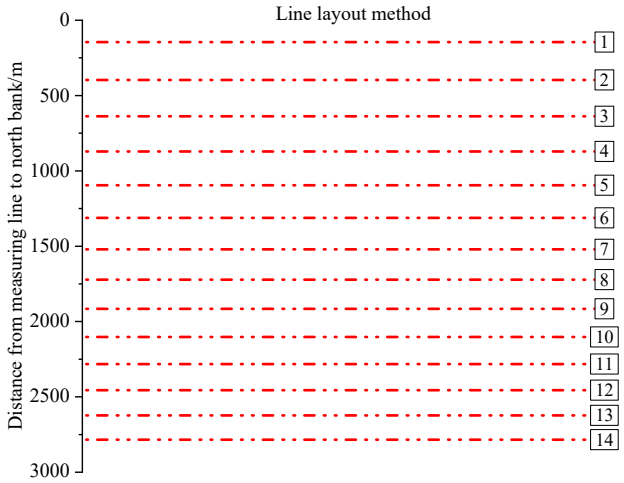

Fig. 22. Simulation Diagram of the Layout of the Survey Line in the First Survey Area

The remaining survey areas will be modeled and solved using the same method as that for the first survey area to obtain the optimal survey line layout for the entire sea area. If the slope in subsequent survey areas is too steep to be approximated to the x- or y-axis, these areas can be further divided into two smaller ones and the same survey line layout method can be applied.

IV. Conclusions

The present study has successfully developed and validated an optimization model for multi-beam bathymetric survey line deployment. Through a systematic three-stage approach, the research has addressed the complexities associated with underwater terrain measurement, leading to significant enhancements in the efficiency and precision of marine surveying operations. The mathematical models and optimization algorithms developed in this study provide a robust framework for minimizing the length of survey lines while maintaining desired coverage width and overlap rates.

In the initial phase, the geometric relationships of an ideal sloping seafloor were leveraged to construct a foundational model for multi-beam coverage width and overlap rate. This was followed by an enhancement of the model to accommodate arbitrary horizontal projection angles, leading to a more generalized and adaptable model for various seabed conditions. The final phase involved partitioning complex seafloor terrains into regular sloped planes, which were then optimized using a single-objective model to explore efficient survey line deployment strategies.

The results, obtained through MATLAB simulations, demonstrated the model's capability to accurately predict water depth, coverage width, and overlap rate under diverse conditions. The visualization of survey line deployment plans further solidified the practical applicability of the model. This research not only offers a theoretical foundation for optimizing multi-beam bathymetric surveying but also presents a practical guide for executing marine surveys with improved efficiency and accuracy.

In conclusion, the optimization model for multi-beam bathymetric survey lines presented in this paper stands as a significant contribution to the field of marine mapping. It provides a systematic approach to navigating the challenges of underwater terrain measurement, ensuring comprehensive coverage, and optimizing resource allocation. The model's effectiveness is evident through its ability to minimize survey line lengths, a critical factor in enhancing survey efficiency and reducing operational costs.

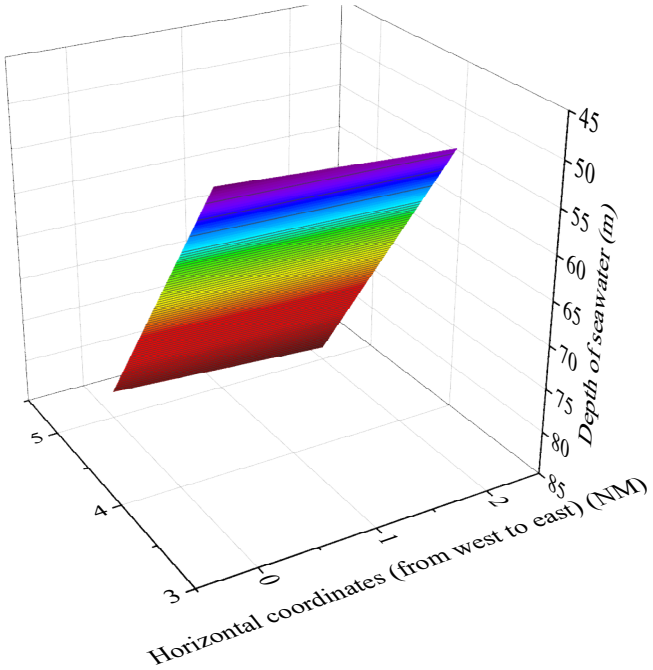

Fig. 23. Fitting Diagram of the First Survey Area

TABLE I
EXAMPLES OF SEA DEPTH, COVERAGE WIDTH, AND OVERLAP RATIO RESULTS AT DIFFERENT DISTANCES

Distance of Survey Line from Center Point/m	-800	-600	-400	-200	0	200	400	600	800
Depth of Sea/m	90.95	85.71	80.47	75.24	70.00	64.76	59.53	54.29	49.05
Coverage Width/m	315.70	297.53	279.35	261.17	242.99	224.81	206.63	188.45	170.27
Overlap Rate with Previous Line/%	——	35.70	31.51	26.74	21.26	14.89	7.41	-1.53	-12.37

TABLE II
COVERAGE WIDTH OF MULTI-BEAM BATHYMETRY AT VARIOUS LOCATIONS

Coverage width/m		Measure the distance of the ship from the center point of the sea /nautical mile							
		0	0.3	0.6	0.9	1.2	1.5	1.8	2.1
Angle of line direction/°	0	415.7	466.1	516.5	566.9	617.3	667.7	718.1	768.5
	45	416.3	452.0	487.7	523.4	559.1	594.8	630.5	666.1
	90	416.4	416.4	416.4	416.4	416.4	416.4	416.4	416.4
	135	415.7	380.1	344.4	308.8	273.1	237.5	201.9	166.2
	180	415.7	365.8	315.3	264.8	214.4	163.9	113.4	63.0
	225	416.4	380.7	345.0	309.3	273.6	237.9	202.2	166.5
	270	416.4	416.4	416.4	416.4	416.4	416.4	416.4	416.4
	315	416.2	451.8	487.5	523.2	558.9	594.6	630.2	665.9

TABLE III
PARTIAL SEA AREA TOPOGRAPHY DATA

The depth of the sea/m		Transverse coordinates/NM（From the West to the East）									
		0.00	0.02	0.04	0.06	0.08	0.10	0.12	0.14	0.16	……
Longitudinal coordinates/NM (From the south to the north)	0.00	24.40	24.12	23.85	23.59	23.34	23.10	22.88	22.67	22.46	
	0.02	24.32	24.04	23.77	23.51	23.27	23.03	22.81	22.60	22.39	
	0.04	24.25	23.97	23.70	23.44	23.19	22.96	22.74	22.53	22.33	……
	0.06	24.17	23.89	23.63	23.37	23.13	22.89	22.67	22.46	22.26	
	0.08	24.10	23.82	23.56	23.30	23.06	22.83	22.61	22.40	22.20	
	0.10	24.03	23.76	23.49	23.24	23.00	22.76	22.55	22.34	22.14	
	……					……					……

TABLE IV
LAYOUT PARAMETERS FOR THE FIRST SURVEY AREA

Line code	Survey line location/m	The depth of sea/m	Survey line coverage width/m	The cumulative coverage width of the survey line/m
1	145.25	82.14	284.65	284.65
2	396.17	79.16	274.33	530.51
3	637.99	76.29	264.38	767.46
4	871.05	73.52	254.79	995.83
5	1095.66	70.86	245.56	1215.91
6	1312.12	68.29	236.65	1428.01
7	1520.73	65.81	228.07	1632.42
8	1721.78	63.42	219.80	1829.42
9	1915.54	61.12	211.83	2019.28
10	2102.27	58.91	204.15	2202.25
11	2282.23	56.77	196.75	2378.58
12	2455.67	54.71	189.62	2548.53
13	2622.82	52.73	182.74	2712.31
14	2783.91	50.82	176.11	2870.16

REFERENCES

[1] F. Cheng and N. Hu, "Research on the optimisation method of multibeam survey line laying," *Journal of Marine Technology,* vol. 35, no. 02, pp. 87-91, 2016.

[2] B. He and X. Cheng, "Application of Multi Wave Beam Sounding System in Sea-Floor Scan Engineering," *Port Sci. Technol.,* no. 05, pp. 23-26, 2012.

[3] Q. Dong, M. Cui, J. Zhou, J. Wang, and Y. Xu, "Analysis and Processing of Transform Geography of Convex and Concave in Multi-beam Sounding System.," *Hydrographic Surv. Charting,* vol. 31, no. 01, pp. 32-35, 2011.

[4] T. Zhang, S. Qin, J. Tang, and X. Wang, "echnical Status and Development Trend of Deep-sea Multi-beam Bathymetry System," *Bull. Surv. Mapp,* no. 05, pp. 82-85, 2018.

[5] X. Wang and H. Xing, "Discussion on the Relation between Space Plane Angles and its Projection," *J. North China Inst. Sci. Technol,* vol. 11, no. 04, pp. 45-48, 2014.

[6] S. Zhang, "Projection Analysis and Research of Arbitrary Plane Angles in Space," *Course Educ. Res,* no. 31, pp. 109-110, 2015.

[7] R. Mi, "Application and accuracy verification of multi-beam bathymetry system for unmanned vessels.," *Survey World,* no. 06, pp. 55-57+64, 2023.

[8] Z. Yang *et al.*, "Application Research of Multi-beam Sounding System in the Field of Underwater Structure Detection," *Guangzhou Archit,* vol. 51, no. 06, pp. 84-86, 2023.

[9] X. Han, "Planar Layout of Multi-beam Surveying in Coastal Engineering Construction," *Jiangxi Surv. Mapp,* no. 04, pp. 19-20, 2013.

[10] Y. Zhu, "Multi-Beam Oceanographic Mapping Analysis Based on Engineering Cases," *Constr. Des. Eng,* no. 20, pp. 238-239, 2020.

[11] S. Liu, "Talks on Guarantee Measures for Surveying Multi-beam in Sallow Water.," *Port Eng. Technol,* no. 02, pp. 52-54, 2007.

[12] J. Wang, Y. Tang, S. Jin, G. Bian, X. Zhao, and C. Peng, "A Method for Multi-Beam Bathymetric Surveys in Unfamiliar Waters Based on the AUV Constant-Depth Mode.," *Journal of Marine Science and Engineering,* vol. 11, no. 7, 2023.

[13] F. Wang and Y. Ma, "Design and realization of line layout system for marine multi-beam bathymetric survey.," *J. Mar. Inf. Technol. Appl,* vol. 38, no. 03, pp. 158-162+186, 2023.

[14] J. Shan, S. Li, Q. Yang, D. Fan, C. Zhang, and Z. Xing, "Combining Satellite Altimetry Technology to Design the Surveying Line Density for Shipborne Sonar Sounding," *J. Geom. Sci. Technol,* vol. 38, no. 05, pp. 454-460+465, 2021.

[15] C. Xu, "Application of multi-beam sounding system in siltation calculation of navigation channel.," *World Geol,* vol. 36, no. 01, pp. 311-315, 2017.

[16] L. Zhang and X. Yin, "Planar Layout of Bathymetric Survey and Trajectory Control Algorithm," *Hydrographic Surv. Charting,* no. 02, pp. 33-35, 2002.

[17] J. Chai, "Study on Sounding Survey Line Planning and Running Strategy," *Hydrographic Surv. Charting,* vol. 33, no. 03, pp. 43-46, 2013.

[18] X. Shi, K. Ji, W. Li, and Y. Yuan, "Application of Multi-Measurement Gross Error Elimination Method Considering Terrain Change inIntegrated Un-derwater Measurement," *J. Ocean Technol,* vol. 38, no. 05, pp. 32-36, 2019.

[19] W. Xia, Y. Liu, F. Xiao, and G. Zhai, "The Effect of the Different Hydrographic General Line Direction on the Seabed Display," *Hydrographic Surv. Charting,* no. 03, pp. 28-31, 2004.

[20] Z. Xiao, "GNSS/Sonar track line layout on the sea surface and research on its influence on seafloor positioning. Shandong University of Technology," Master's degree student, 2023.

[21] F. Cheng and M. Zhang, "Research on the Optimization Method for Survey Line Layout in Side Scan Sonar Based on the TargetDetection," *Ship Electron. Eng,* vol. 42, no. 03, pp. 176-178+196, 2022.

[22] Z. Bai, H. Xiao, W. Yan, Y. Cao, and Y. Zou, "Method of Segmented Scanning Planning Line Based on Complex Mountain Digital Elevation Data," in *2021 Geophysical Exploration Seminar of China Petroleum Institute*, Chengdu, Sichuan, China, 2021, p. 4.

[23] S. Jin, J. Li, Z. Wu, G. Bian, and Y. Cui, "Estimation of Spacing of Survey Line Layout with EGM2008 Model in Marine Gravity Survey," *J. Wuhan Univ. (Inf. Sci.),* vol. 43, no. 09, pp. 1315-1319, 2018.

[24] L. Qi, R. Zhai, and A. Li, "A Thinning Algorithm of Multi-beam Sounding Data Considering Slope and Elevation.," *J. Geo-inform. Sci,* vol. 25, no. 01, pp. 142-152, 2023.

[25] Q. Yu, "Seabed Topography Measurement Based on Multi-beam Bathymetry Technology," *Geomatics & Spatial inform. Technol,* vol. 45, no. 09, pp. 262-264, 2022.

[26] F. Zhou, B. Xu, and X. Zhao, "Depth bias model based on artificial neural networks for airborne LiDAR bathymetry," *Hydrographic Surv. Charting,* vol. 42, no. 03, pp. 5-8, 2022.

[27] Q. Xue, "Construction of Seabed 3D Terrain Model based onMulti-beam Sonar Data. Jiangsu Ocean University," Master's degree student, 2022.

[28] M. Li, "Analysis of Bathymetric Survey Techniques in Marine Surveying.," *Technol. Innov. Appl,* vol. 12, no. 34, pp. 185-188, 2022.

[29] S. Shu and L. Cheng, "Application Analysis of Multi-beam System in Yangtze River Channel Surveying," *China Water Transp,* no. 09, pp. 46-47, 2017.

[30] H. Zhu, "Key Technologies and Accuracy Assessment of Underwater Topographic Survey with Multi-beam Bathymetric System," *Survey World,* no. 02, pp. 4-6, 2022.